Cryo-Balloon Catheter Position Planning using AFiT

Andreas Kleinoeder[a], Alexander Brost[a*], Felix Bourier[b], Martin Koch[a], Klaus Kurzidim[b], Joachim Hornegger[ad] and Norbert Strobel[c]

[a]Pattern Recognition Lab, Friedrich-Alexander-University Erlangen-Nuremberg, Erlangen, Germany

[b]Klinik für Herzrhythmusstörungen, Krankenhaus Barmherzige Brüder, Regensburg, Germany

[c]Siemens AG, Healthcare Sector, Forchheim, Germany

[d]School in Advanced Optical Technologies (SAOT), Erlangen, Germany

[*]E-Mail: Alexander.Brost@cs.fau.de

Abstract. Atrial fibrillation (AFib) is the most common heart arrhythmia. In certain situations, it can result in life-threatening complications such as stroke and heart failure. For paroxysmal AFib, pulmonary vein isolation (PVI) by catheter ablation is the recommended choice of treatment if drug therapy fails. During minimally invasive procedures, electrically active tissue around the pulmonary veins is destroyed by either applying heat or cryothermal energy to the tissue. The procedure is usually performed in electrophysiology labs under fluoroscopic guidance. Besides radio-frequency catheter ablation devices, so-called single-shot devices, e.g., the cryothermal balloon catheters, are receiving more and more interest in the electrophysiology (EP) community. Single-shot devices may be advantageous for certain cases, since they can simplify the creation of contiguous (gapless) lesion sets around the pulmonary vein which is needed to achieve PVI. In many cases, a 3-D (CT, MRI, or C-arm CT) image of a patient's left atrium is available. This data can then be used for planning purposes and for supporting catheter navigation during the procedure. Cryo-thermal balloon catheters are commercially available in two different sizes. We propose the Atrial Fibrillation Planning Tool (AFiT), which visualizes the segmented left atrium as well as multiple cryo-balloon catheters within a virtual reality, to find out how well cryo-balloons fit to the anatomy of a patient's left atrium. First evaluations have shown that AFiT helps physicians in two ways. First, they can better assess whether cryo-balloon ablation or RF ablation is the treatment of choice at all. Second, they can select the proper-size cryo-balloon catheter with more confidence.

Keywords: Atrial Fibrillation, Visualization, Catheter Ablation Planning, Electrophysiology, Cryo-balloon

1 DESCRIPTION OF PURPOSE

As atrial fibrillation (AFib) is the most common heart arrhythmia [1], a lot of clinical and technical research focuses on how to improve the treatment further. In the past decade, pulmonary vein isolation (PVI) by catheter ablation has proven to be a safe and effective approach for dealing with paroxysmal AFib [2, 3]. The goal of PVI is the electrical isolation of the left atrium (LA) from the pulmonary veins (PVs) to prevent propagation of electrical signals, which do not belong to the heart conduction system, from the PVs into the left atrium (LA). Isolation is achieved by creating a contiguous transmural lesions around the PVs with an ablation catheter. Besides radio-frequency (RF) catheter ablation which is currently the most common method, the use of single-shot devices is increasing. Compared to a point-by-point RF ablation strategy,

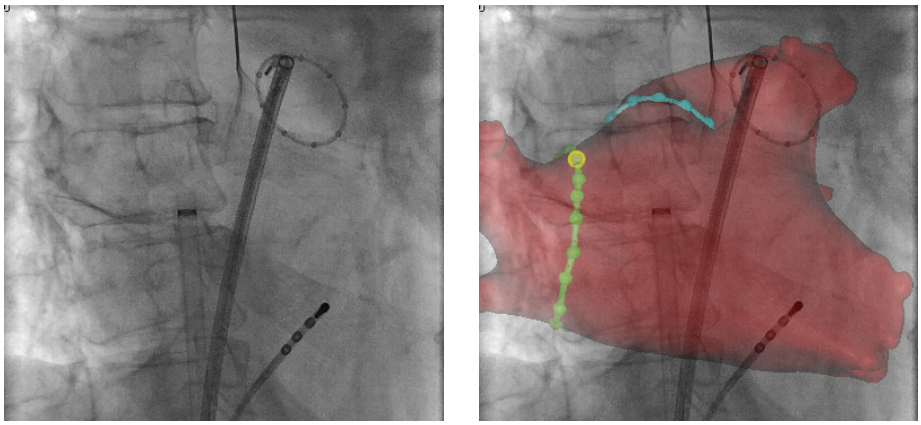

(a) (b)

Figure 1: (a) Fluoro image without overlay image (acquired on an Artis zee Biplane, Siemens AG, Healthcare Sector, Forchheim, Germany). (b) Same fluoro image with overlayed 3-D information obtained by segmenting an MRI data set of a patient's left atrium (LA). The segmented mesh of the LA in combination with previously planned ablation lines is superimposed onto the fluoroscopic X-ray image to provide additional 3-D information during an AFib case.

cryothermal balloon catheters may generate contiguous transmural ablation lines more readily [4]. There is already navigation support for the intervention. As shown in Figure 1, for example, 3-D information of the left atrium including marked regions for 3-D ablation lines can be superimposed onto 2-D live X-ray images [5]. Catheter tracking and object reconstruction from two views can help the user to evaluate how well a device was placed [6, 7]. Moreover, cardiac and respiratory motion can be compensated for by catheter tracking as proposed by Brost *et al.* [8]. Tools for the pre-procedural planning phase, however, are less common. In this paper, we propose a solution to this problem designed to support cryo-balloon ablation procedures. The acquired 3-D model of the LA cannot only be applied to fluoro overlay navigation, but it can also be used for inspection of the anatomical structure during a planning phase [9]. Although tools which can visualize such anatomical models are available, most of them only provide simple measurement routines. In particular, when physicians have to decide which catheter size fits best for a patient, an intuitive visualization of both - the left atrium and the catheter - is desirable. This is why we propose to display a mesh of a segmented LA together with cryo-balloon catheter models of different sizes. Our Atrial Fibrillation planning Tool (AFiT), introduced recently [10], provides interaction between these objects. In this paper we explain the visualization of the segmented left atrium and of the cryo-balloons in more detail.

2 METHODS

For physicians, who consider the use of cryo-balloons, it is not always easy to decide whether cryo-balloon ablation should be the therapy of choice at all. If it is, then they need to find out which catheter size fits best. The anatomy of the pulmonary veins play an important role to make these decisions. For example, the ostium of a PV might be too small or too large for effective cryo-balloon treatment. In such cases, it may be preferable to perform a standard RF-catheter ablation instead. Without pre-operative evaluation, a cryo-balloon might be inserted into the LA only to find out that this device turned out to be suboptimal to treat the PV anatomy at hand. Such a mis-judgement may increase the overall procedure time and cost. In addition, there can be special anatomical configurations that may get in the way when working with cryo-balloon catheters. One would expect that there are always four PV ostia connected to the LA.

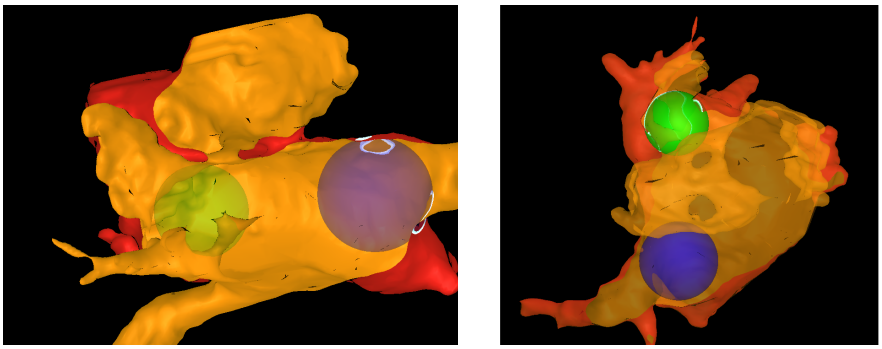

(a) (b)

Figure 2: (a) Multiple cryo-balloons are displayed within the left atrium. The green one represents a balloon with a diameter of 23 mm, the blue one has a diameter of 28 mm. Carving is set to its maximum and each catheter has an individual transparency. (b) To verify the catheters' positions the camera has been rotated to an posterior-anterior view.

Unfortunately, there are anatomical variations where two PVs form what is called a *common ostium*. In such a case, both PVs are very close to each other and effectively merge into one bigger ostium. In such a case, physicians may have to apply two 'shots' - one for the upper pulmonary vein and one for the lower - to create a lesion. However, it can not be guaranteed that these two shots will create a gapless lesion around the PVs. If the PVs are not connected to each other, there still remains the question of the appropriate catheter size. This section describes several functionalities of AFiT which help the physician to make informed treatment decisions ahead of an actual case.

2.1 Catheter Visualization

After the trans-septal puncture of the inter-atrial septum, physicians can navigate the ablation and mapping catheters inside the left atrium. When the cryo-balloon catheter has reached the LA, it can be inflated to its full size, and then be pressed against the ostium of the pulmonary vein. Cryo-balloon catheters are currently available with diameters of 23 mm and 28 mm. When the full size of a balloon catheter is reached, the catheter is almost of spherical shape. Thus, for visualization of cryo-balloons, a sphere with two possible diameter, 23 mm and 28 mm, is used. In addition, multiple balloon catheters can be visualized at the same time and the size of each can be switched between 23 mm and 28 mm. Fig. 2 shows how two different balloon-catheters are rendered inside the LA. Arbitrary rotation of the left atrium combined with a picking function for the catheter objects allow an intuitive placement of the cryo-balloon.

2.2 Transparency

To provide a better impression of the single catheter position in the LA, the transparency of each object can be adjusted separately. The physician can adjust the transparency of the LA as well as the transparency of all cryo-balloons individually. Transparency is important when two catheter models are positioned close to each other. In this case, activated transparency prevents mutual occlusion between two catheters. In addition, the user can still see behind the placed catheters which improves spatial perception. Since the rendered objects are more complex than in usual rendering scenes, rendering different transparencies was solved by a technique called *dual depth-peeling* [11]. To display a correct transparency of the objects, all transparent objects usually have to be ordered from front to back from the cameras viewpoint. If sorting is not considered, wrong results can occur, see Figure 3 for an example. Sorting is a common method used for correct transparency but because of the complexity of the scene objects in

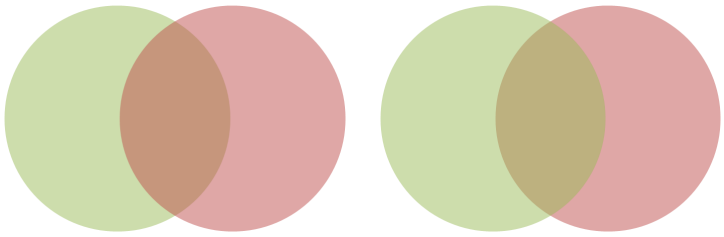

(a) (b)

Figure 3: Both circles have a transparency of 50%.(a) The red circle is in front of the green circle. (b) The green circle is in front of the red circle. The resulting color of the intersecting area from the two circles depend on the order of the objects. Thus, objects should be sorted to gain a correct result.

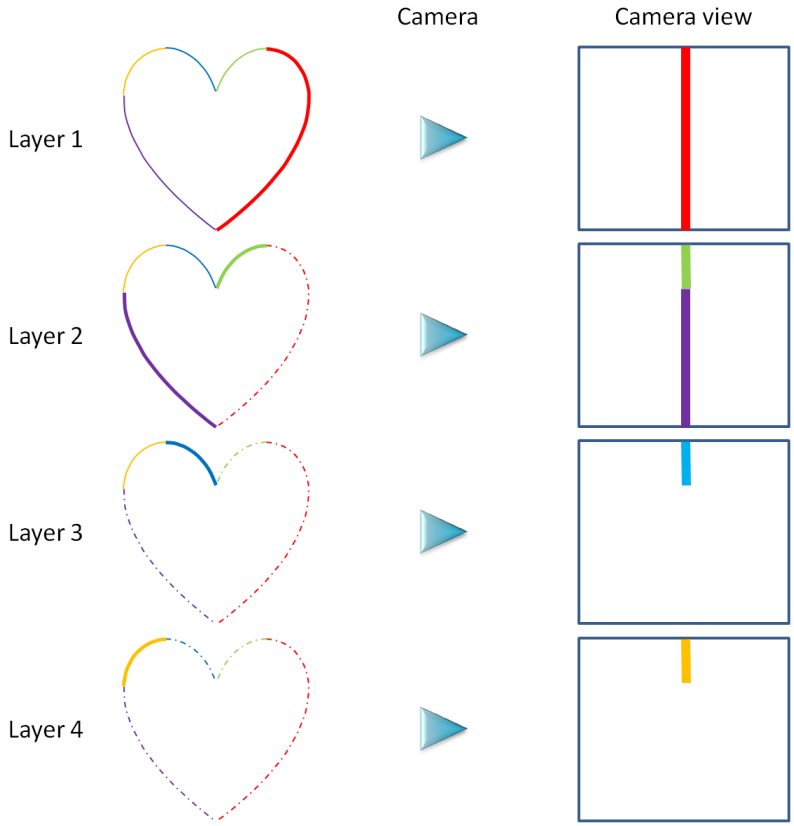

Figure 4: The bold lines represent the current layer, i.e. the layer which is visible to the viewer. The thin lines are occluded layers which are currently not visible. The dash-dotted thin lines are layers which already have been peeled away by the algorithm. In each iteration the previous layer is used for peeling such that the layer behind becomes visible.

AFiT, such an approach would cause too much computing overhead. Each object - the LA and each cryo-balloon - consists of a certain amount of triangles which would have to be sorted w.r.t. each other. The depth-peeling approach is an order-independent algorithm which is capable of rendering a scene with correct transparency without the need of sorting polygons [12]. The idea of this technique is to extract, store and finally blend different depth layers of the scene. In the first step, the scene is rendered as usual to receive the first layer. To get the second layer, the depth information of the first layer is used to peel away the pixels which occlude layer two. This peeling is repeated in sequential render passes until all depth layers have been found. The

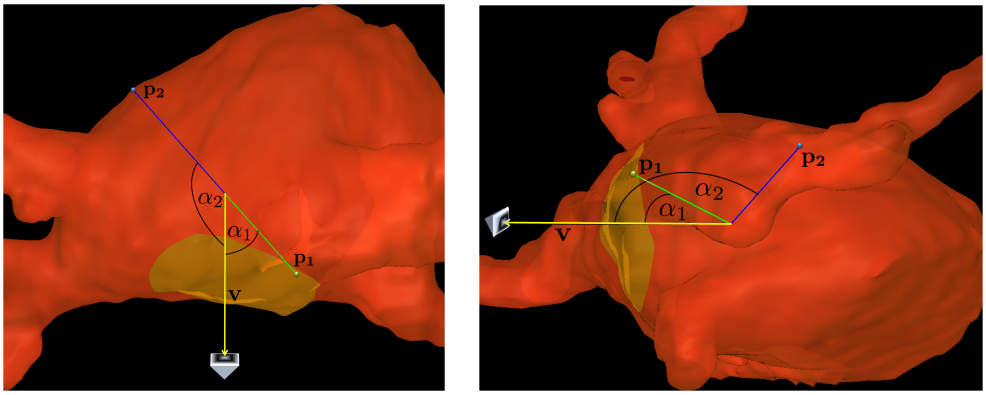

(a) (b)

Figure 5: The yellow arrow points to the viewing direction $\mathbf{v}$. The green and blue line each represent one pixel direction $\mathbf{p_1}$ and $\mathbf{p_2}$. The angle α_1 is smaller than β, thus $\mathbf{p_1}$ is not drawn. $\mathbf{p_2}$ however is drawn because of a bigger angle α_2.(a) View from top of camera. (b) View from right hand side of camera.

final scene then can be calculated by blending all the layers together in the same order they have been obtained. As an example Figure 4 illustrates depth-peeling in a simple 2-D sketch. This technique finds its application in several topics of computer graphics such as smooth shadow mapping [13], volume rendering [14] and ray-casting [15]. The drawback of this approach is that for each layer the whole scene has to be redrawn which results into N render passes for N layers. This may slow down the frame rate of the application if too many layers need to be computed. During dual depth-peeling, the front and back layers can be peeled simultaneously such that the only N/2+1 passes are needed [11]. Additionally, the number of render passes can manually be restricted to a maximum. But this may result into wrong transparency effects in the rear locations of the scene which is considered to be acceptable.

2.3 View Inside the Left Atrium

Planning of the procedure needs to be simplified as well as the assessment if the size of a cryo-balloon catheter can be used for the pulmonary vein considered for ablation. To provide physicians a view inside the LA, the mesh representation can be literally cut open. A slider regulates the expansion of the opened mesh which propagates from the middle of the model to the border of the model. In the following this effect is denoted as *carving*. To gain an intuitive behavior of the carving effect, the front-facing part of the left atrium has to be set partially invisible depending on how high the carving-factor is set by the user. During the development of AFiT several approaches have been tested. The current and at this point most appropriate implementation will be described in the following. We will briefly describe the implementation of the algorithm. The camera model is configured as an orthographic projection, i.e., that objects which are further away will not appear smaller during rendering. The optical center $\mathbf{c} = (c_x, c_y, c_z)^\top \in \mathbb{R}^3$ is positioned in a fixed depth of the scene and can only be moved in x- and y- direction. The viewing direction $\mathbf{v} \in \mathbb{R}^3$ is also fixed to look along the positive z-axis, $\mathbf{v} = (0, 0, 1)^\top$. The triangle-mesh of the LA is centered around the origin. In world-space, each pixel of the mesh can be described as a vector $\mathbf{p} = (p_x, p_y, p_z)^\top \in \mathbb{R}^3$ which represents the coordinates of the pixel from the origin. Normalization of $\mathbf{p}$ yields $\hat{\mathbf{p}} \in \mathbb{R}^3$, i.e.

$$\hat{\mathbf{p}} = \frac{\mathbf{p}}{||\mathbf{p}||_2}. \tag{1}$$

The angle α between the viewing direction $\mathbf{v}$ and the direction of a pixel $\mathbf{p}$ can be calculated by

$$\alpha = \arccos(\mathbf{v} \cdot \hat{\mathbf{p}}). \tag{2}$$

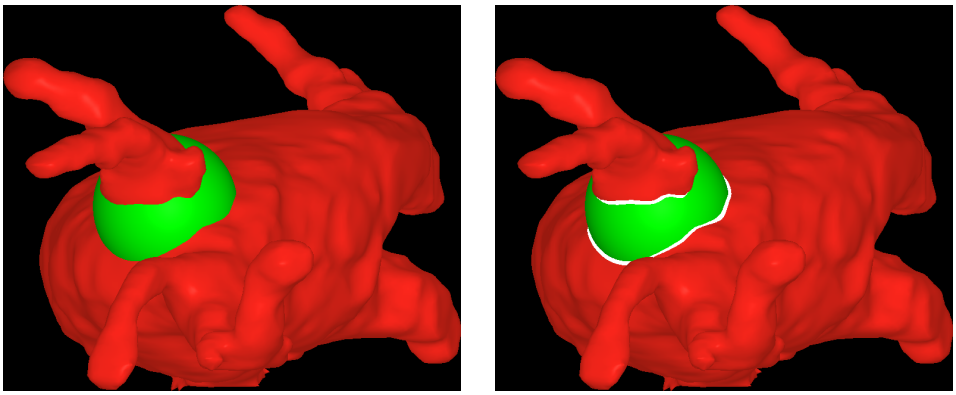

(a) (b)

Figure 6: Cryo-balloon positioned at one of the pulmonary veins inside the LA. (a) Intersection line is turned off. (b) Intersection line is turned on.

An angle α_i is calculated for each pixel $\mathbf{p}_i$ with $i \in [1, M]$ where M is the number of mesh pixels generated during rendering. These angles now can be compared to a fixed angle β which is set by the user. If the pixels' angle α_i is smaller than β, the pixel will not be drawn. Figure 5 illustrates this calculation. The carving effect was implemented using shaders [16]. The use of shaders allows to render more flexible computer graphics compared to the fixed-function pipeline. Shaders are already well known and are commonly used in the field of computer graphics. Since carving should take effect on per pixel basis, the calculation is processed in the pixel shader which is also often referred to as fragment shader.

2.4 Intersection Catheter and Left Atrium

The tool operates with a rigid model of the left atrium. Deformation due to the cryo-balloon would be possible, but requires more knowledge of the underlying physical model as well as the information, how the left atrium itself changes due to cardiac motion. Nevertheless, a visualization of how well a catheter fits to a pulmonary vein is desirable. As a first approach, we propose to visualize the intersection lines caused by the cryo-balloon and the left atrium. The intersection is displayed on the surface of the left atrium since this is the object which is of interest for the physician. By comparing the intersection lines at different positions and sizes of the cryo-balloon, the most suitable catheter size can be determined. The line interactively moves with the position of the catheter as the intersection is calculated on the fly. Again, the calculation of the intersection line takes place in the fragment shader. To be able to calculate where the cryo-balloon is intersecting the LA, the cryo-balloon's midpoint $\mathbf{m} \in \mathbb{R}^3$ and the radius $r \in \mathbb{R}$ have to be known while the LA is drawn. In a first step, the distance $d \in \mathbb{R}$ of the currently processed pixel $\mathbf{p}$ to the cryo-balloons midpoint is calculated by

$$d = ||\mathbf{p} - \mathbf{m}||_2. \tag{3}$$

Due to numerical limited precision the exact calculation of intersecting pixels will not happen often. By defining an offset $\varepsilon \in \mathbb{R}$, it can be evaluated if the calculated distance d is close to r. A point of the mesh will be considered as intersection point if the following condition holds

$$|d - r| < \varepsilon. \tag{4}$$

3 RESULTS

A first practical evaluation of this tool obtained a very positive feedback. The software could greatly support physicians during the planning phase. The look and feel turned out to be well

and a decision about a suitable balloon size could be found much faster than before. A valid evaluation and more results require a patient study, which is currently in preparation.

4 CONCLUSION

Our software is able to support physicians during the planning phase. In particular, when uncertainties during catheter selection occur, AFiT helps during the decision finding process. The multiple visual effects, in addition to a freely placeable catheter model, make this tool unique for the pre-procedural planning phase. First evaluations have shown that this tool can simplify the planning phase, particularly when it comes to the decision about the catheter size. AFiT could further be extended by adding other catheter models as well.

Acknowledgements

This work has been supported by the German Federal Ministry of Education and Research (BMBF), project grant No. 01EX1012E, in the context of the initiative Spitzencluster Medical Valley - Europäische Metropolregion Nürnberg. Additional funding was provided by Siemens AG, Healthcare Sector.

References

[1] H. Calkins, J. Brugada, D. Packer, R. Cappato, S.-A. Chen, H. Crijns, R. Damiano, D. Davies, D. Haines, M. Haissaguerre, Y. Iesaka, W. Jackman, P. Jais, H. Kottkamp, K. Kuck, B. Lindsay, F. Marchlinski, P. McCarthy, J. Mont, F. Morady, K. Nademanee, A. Natale, C. Pappone, E. Prystowsky, A. Raviele, J. Ruskin, and R. Shemin, "HRS/EHRA/ECAS Expert Consensus Statement on Catheter and Surgical Ablation of Atrial Fibrillation: Recommendations for Personnel, Policy, Procedures and Follow-Up," *Heart Rhythm* **4**, 1–46 (2007).

[2] V. Fuster, L. Rydén, D. Cannom, H. Crijns, A. Curtis, K. Ellenbogen, J. Halperin, J.-Y. L. Heuzey, G. K. J. Lowe, S. Olsson, E. Prystowsky, J. Tamargo, S. Wann, S. Smith, A. Jacobs, C. Adams, J. Anderson, E. Antman, J. Halperin, S. Hunt, R. Nishimura, J. Ornato, R. Page, B. Riegel, S. Priori, J.-J. Blanc, A. Budaj, A. Camm, V. Dean, J. Deckers, C. Despres, K. Dickstein, J. Lekakis, K. McGregor, M. Metra, J. Morais, A. Osterspey, J. Tamargo, and J. Zamorano, "ACC/AHA/ESC Practice Guidelines," *Circulation - Journal of the American Heart Association* **114**, 258 – 354 (2006).

[3] A. Natale, A. Raviele, A. Al-Ahmad, O. Alfieri, E. Aliot, J. Almendral, G. Breithardt, J. Brugada, H. Calkins, D. Callans, and et al., "Venice chart international consensus document on ventricular tachycardia/ventricular fibrillation ablation.," *Journal of Cardiovascular Electrophysiology* **21**(3), 339–379 (2010).

[4] T. Neumann, J. Vogt, B. Schumacher, A. Dorszewski, M. Kuniss, H. Neuser, K. Kurzidim, A. Berkowitsch, M. Koller, J. Heintze, U. Scholz, U. Wetzel, M. Schneider, D. Horstkotte, C. Hamm, and H.-F. Pitschner, "Circumferential Pulmonary Vein Isolation With the Cryoballoon Technique Results From a Prospective 3-Center Study," *Journal of the American College of Cardiology* **52**, 273 – 278 (2008).

[5] J. Ector, S. D. Buck, W. Huybrechts, D. Nuyens, S. Dymarkowski, J. Bogaert, F. Maes, and H. Heidbüchel, "Biplane three-dimensional augmented fluoroscopy as single navigation tool for ablation of atrial fibrillation: Accuracy and clinical value," *Heart Rhythm* **5**, 957–964 (2008).

[6] A. Brost, R. Liao, J. Hornegger, and N. Strobel, "3-D Respiratory Motion Compensation during EP Procedures by Image-Based 3-D Lasso Catheter Model Generation and Tracking," in *MICCAI 2009, London, UK, LNCS* **5761**, 394–401, Springer Berlin / Heidelberg (2009).

[7] A. Kleinoeder, A. Brost, F. Bourier, M. Koch, K. Kurzidim, J. Hornegger, and N. Strobel, "Cryo-Balloon Reconstruction from Two Views," in *to appear in ICIP 2011*, (Bruessels, Belgium) (September, 2011).

[8] A. Brost, A. Wimmer, R. Liao, J. Hornegger, and N. Strobel, "Constrained 2-D/3-D Registration for Motion Compensation in AFib Ablation Procedures," in *IPCAI 2011, Berlin, Germany*, *LNCS* **6689**, 133–144, Springer Berlin / Heidelberg (2011).

[9] J. Ector, S. D. Buck, S. Dymarkowski, J. Bogaert, F. Maes, and H. Heidbüchel, "MRI-based 3D modelling of the right atrium allows for pre-procedural ablation planning," *European heart journal* **26**, 297 (2005).

[10] A. Brost, F. Bourier, A. Kleinoeder, J. Raab, M. Koch, M. Stamminger, J. Hornegger, N. Strobel, and K. Kurzidim, "Afit - atrial fibrillation ablation planning tool'," in *to appear in VMV 2011*, (Berlin, Germany) (October, 2011).

[11] L. Bavoil and K. Meyers, "Order Independent Transparency with Dual Depth Peeling," (2008).

[12] C. Everitt, "Interactive order-independent transparency," tech. rep., NVIDIA Corporation (2001).

[13] L. Bavoil, S. P. Callahan, and C. T. Silva, "Robust soft shadow mapping with depth peeling," tech. rep., Scientific Computing and Imaging Institute University of Utah, Salt Lake City, UT 84112 USA (2006).

[14] D. Borland, J. P. Clarke, and M. T. I. Russell, "Volumetric depth peeling for virtual arthroscopy," *Electronic Imaging* **16**(2) (2005).

[15] F. F. Bernardon, C. A. Pagot, J. L. D. Comba, and C. T. Silva, "Gpu-based tiled ray casting using depth peeling.," *Journal of Graphics Tools* **11.3**(ISSN 1086-7651), 23–29 (2006).

[16] R. J. Rost, *OpenGL(R) Shading Language (2nd Edition)*, Addison-Wesley Professional (2006).